Cement and Concrete Research 185 (2024) 107631

Contents lists available at ScienceDirect

Cement and Concrete Research

journal homepage: www.elsevier.com/locate/cemconres

# The manufacture of natural hydraulic limes: Influence of raw materials' composition, calcination and slaking in the crystal-chemical properties of binders

C. Parra-Fernández [a], A. Arizzi [a,*], M. Secco [b], G. Cultrone [a]

[a] Universidad de Granada, Departamento de Mineralogía y Petrología, Campus Fuentenueva s/n, 18002 Granada, Spain
[b] Università degli Studi di Padova, Dipartimento dei Beni Culturali (dBC), Piazza Capitaniato 7, 35139 Padova, Italy

ARTICLE INFO

*Keywords:*
Hydraulicity
Reactive silica
Calcium silicates
Portlandite
Air exposure

ABSTRACT

This study aims to achieve an in-depth understanding of the manufacturing process of natural hydraulic lime (NHL) by assessing the influence of raw materials' chemical- mineralogical composition and the effect of the slaking process. NHLs with variable hydraulicity were manufactured using 56 raw materials from carbonate outcrops in Andalusia (Spain). This study shows that siliceous limestones with microcrystalline quartz generate hydraulic phases after calcination. However, when the amount of this reactive silica exceeds 18% by weight, CaO is not formed, and only calcium silicates appear. It was also found that slaking of NHL leads to partial hydration of the most reactive calcium silicates, reducing the expected reactivity of the lime. Instead, exposure of NHL quicklimes to environmental relative humidity promotes the formation of disordered portlandite and reduces the partial hydration of hydraulic phases. Our findings demonstrate that standard slaking can be replaced by alternative methods for the studied binders.

## 1. Introduction

Natural hydraulic limes (NHLs) are binders obtained from the calcination of limestone with silica and aluminium impurities at temperatures lower than 1250 °C. Previous scientific research indicates that only marly limestones or limestones with a certain clay content are suitable to produce hydraulic binders, being the clay content the responsible for the hydraulicity of the lime [1–4]. It is known that the initial clay content for the production of natural hydraulic limes is approximately 8% by weight for feebly hydraulic limes (NHL2), 15% for intermediate hydraulic limes (NHL3.5), and 25% for eminently hydraulic limes (NHL5) [1–4].

During the calcination process, and after thermal decomposition of the calcium carbonate into calcium oxide (CaO) and carbon dioxide ($CO_2$), a solid-state reaction takes place among CaO and $SiO_2$, $Al_2O_3$ and $Fe_2O_3$ oxides, released by clays' decomposition [1,2,5–8]. These reactions lead to the formation of calcium silicates and aluminates, whose composition and amount vary depending on the raw material and the calcination conditions in the kiln (temperature, duration of the process and the $CO_2$ partial pressure [9]), thus conferring different properties to the NHL, such as hydraulic reactivity and degree of hydraulicity [1,10–13].

The most remarkable properties of a quicklime (i.e. the calcined raw material) for the obtention of suitable NHL are high hydraulic reactivity, large specific surface area and low density. According to Carran et al. [11] (after the reactivity test, EN 459–2 [14]) and Afridi et al. [15], the most reactive quicklimes are achieved with calcination temperatures from 900 to 1100 °C and dwell times of 3-4 h. Higher calcination temperatures and longer dwell times in the kiln would be detrimental [10,16], as calcium oxide particles or crystals tend to increase in size, agglomerate and partially sinter, leading to a reduction in specific surface area and porosity as bulk density increases [10,16], with negative consequences for the slaking process. Moreover, higher calcination temperatures would enhance the formation of the silicate phases, reducing the amount of free CaO [7].

Another aspect to be considered about the calcination process is that the temperature reached in the kiln may not be homogeneous, having low-temperature points where thermal decomposition of calcite cannot occur (600–900 °C [17]), with an influence not only on the reactivity of NHL, but also on its plasticity (related to mortar's workability), due to the grain size and morphology of the unburnt calcite [18]. At the same time, high temperature points known as *hot spots* might be present in the

* Corresponding author.
*E-mail address:* arizzina@ugr.es (A. Arizzi).

https://doi.org/10.1016/j.cemconres.2024.107631
Received 7 May 2024; Received in revised form 17 July 2024; Accepted 1 August 2024

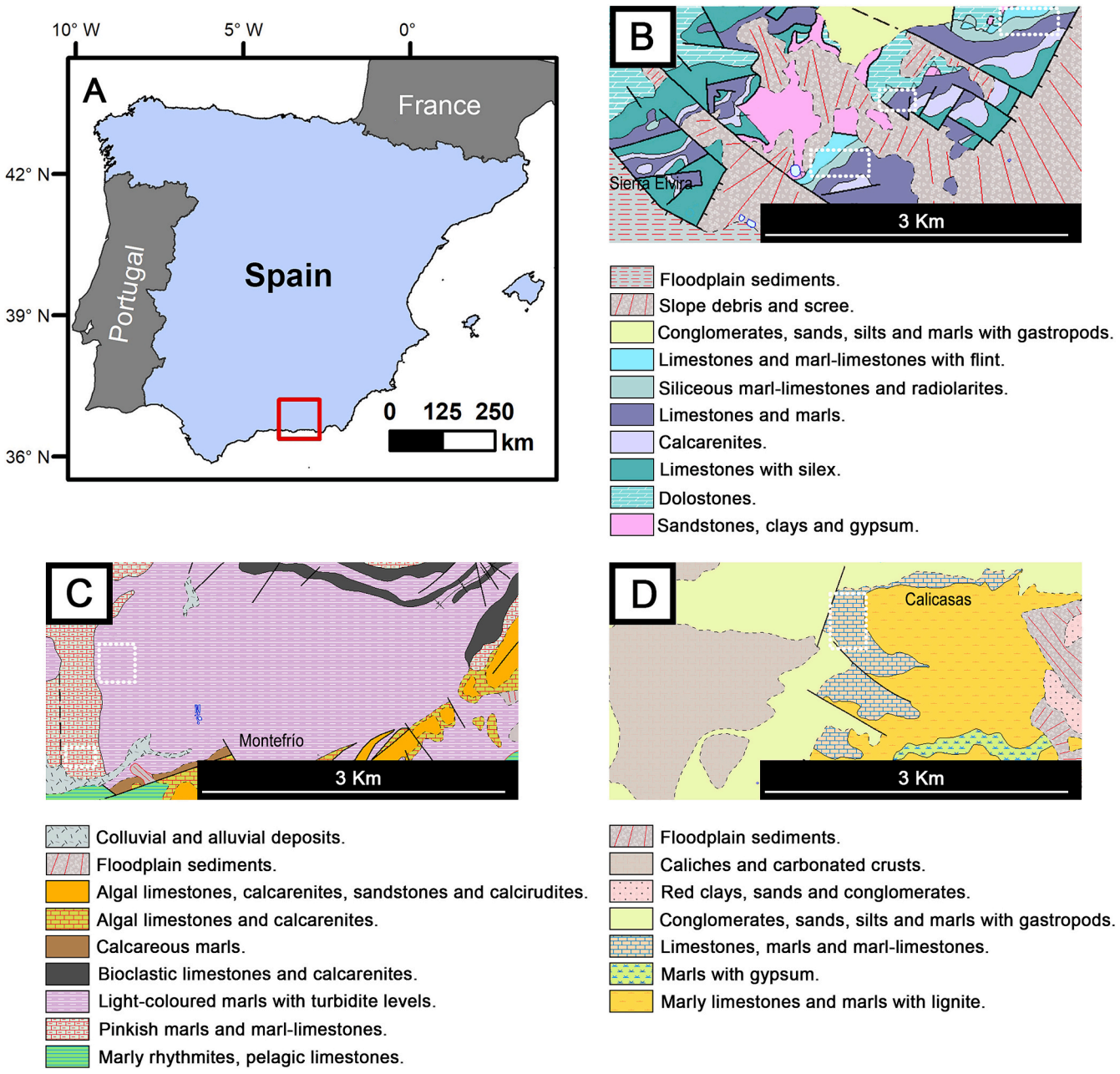


**Fig. 1.** A) Map of the Iberian Peninsula showing within the red box the location of sampling areas; B), C) and D) geological context of the sampled areas (*Sierra Elvira*, *Montefrío* and *Calicasas*, respectively) modified from the Geological Map of Spain ArcGis Web map at a scale of 1:50.000 [44]. Sampling areas are marked by white dashed rectangles. Black lines correspond to tectonic structures such as faults, thrusts, and fold axes. (For interpretation of the references to colour in this figure legend, the reader is referred to the web version of this article.)

kiln, promoting the formation of high-temperature hydraulic phases, such as *alite* ($C_3S$, according to the cement notation) [19].

Overall, these factors influence the duration of the setting process of natural hydraulic limes [2,20–25] and, therefore, the physical and mechanical properties of the final mortar [3,26].

It is evident that the chemical-mineralogical composition of raw materials and manufacturing conditions in the kiln are two key aspects for the correct classification of natural hydraulic limes. Notwithstanding, the current European specifications on building limes (EN 459–1 [27]) does not precisely define chemical and mineralogical requirements for raw materials but, instead, classifies these limes mainly on the basis of the mechanical resistance of NHL mortars after 28 days of curing. This implies that natural hydraulic limes with very different compositional and textural characteristics may fall in the same NHL class (NHL 2, NHL 3.5, or NHL 5 according to the EN 459–1 [27]), with negative consequences on the expected behaviour on site.

The research carried out during the last decades has already highlighted the lack of chemical and mineralogical information in the classification of limes with hydraulic properties [7,13,28–33]. Moreover, due to the widely recognised influence of the calcination process on the reactivity of NHL [34,35], research studies have been extensively focused at establishing a suitable temperature range to achieve optimum NHL quicklime [7,33]. Nevertheless, little is known about the influence of the slaking process in the final properties of natural hydraulic limes, as this aspect has not been sufficiently addressed in literature so far.

Based on these premises, this research work seeks to promote an increased knowledge on natural hydraulic limes, from the selection of compositionally suitable raw materials to the achievement of an

optimum manufacturing process for the obtention of NHLs that can be clearly differentiated and classified. As a reference, the laboratory-manufactured NHLs have been compared to two types of commercial NHLs.

## 2. Materials and methods

### 2.1. Raw materials: sampling and characterization

#### 2.1.1. Sampling areas

Raw materials from different outcrops in the province of Granada (Andalusia, Spain) were sampled. These geological areas were previously identified by Rodríguez Ávila [36] as potentially exploitable outcrops to produce hydraulic binders based on the hydraulicity index (HI, according to Boynton [37]). Thus, some of these outcrops had already been exploited in the past for this aim, although today production plants are not active anymore [38,39]. 56 samples were taken from *Sierra Elvira*, *Montefrío* and *Calicasas* areas (Fig. 1). Geologically, raw materials from *Sierra Elvira* correspond to levels of marl-limestones, marls and nodulous limestones from the Domeriense-Toarciense, siliceous marl-limestones and radiolarites from the Dogger, and limestones and marl-limestones with flint from the Malm. Samples from *Montefrío* are mainly pinkish marls and marl-limestones from the Senoniense-Paleogene and light-coloured marls with turbidite levels from the Oligocene. Those from *Calicasas*, in the Depression of Granada, are mostly limestones, marls and marl-limestones from the Neogene [40–43].

#### 2.1.2. Chemical-mineralogical and petrographic study of raw materials

The chemical analysis of raw materials has been performed using X-ray fluorescence (XRF), by means of a S4 Pioneer-Bruker wavelength dispersive X-ray fluorescence spectrometer, with a Rh tube (60 kV; 150 mA), LIF200/PET/OVO-55 analyser crystals and gas-flow proportional and scintillation detectors. Samples were ground and dispersed in potassium bromide tablets before the analysis. Measurements were taken in vacuum on rotating samples, in order to obtain a quantification of major elements (expressed as oxides), used for the calculation of the cementation index (CI) (Eq. (1)) and other chemical criteria set out in previous scientific papers [1–4,37,45].

$$CI = \frac{2.8\ (\%SiO_2) + 1.1\ (\%Al_2O_3) + 0.7\ (\%Fe_2O_3)}{(\%CaO) + 1.4\ (\%MgO)} \quad (1)$$

Qualitative X-Ray diffraction (XRD) analyses were carried out with an X'Pert Pro Diffractometer equipped with continuous sample rotation system using the disordered crystalline powder method. The experimental conditions were as follows: voltage of 45 kV; current of 40 mA; CuKα radiation (λ = 1.5405 Å); explored area between 4° and 70° 2θ; goniometer speed of 0.1° 2θ/s. Data were interpreted using the X'pert Highscore Plus 4.9 software (Panalytical).

For the quantification of crystalline and amorphous phases in a selection of suitable raw materials, 20 wt% of ZnO was added to the powders as internal standard. Data were collected using a Bragg–-Brentano θ–θ diffractometer (Panalytical X'Pert Pro, CoKα radiation (λ = 1.7889 Å), 40 kV and 40 mA) equipped with a real-time multiple strip (RTMS) detector (X'Celerator by Panalytical). Data acquisition was performed by operating a continuous scan in the range 3–85° 2θ, with a virtual step scan of 0.02° 2θ. Diffraction patterns were interpreted using the X'Pert HighScore Plus 3.0 software by Panalytical, qualitatively reconstructing mineral profiles of the compounds by comparison with PDF databases from the International Centre for Diffraction Data (ICDD). Then, mineralogical quantitative phase analyses (QPA) based on the Rietveld method [46] was performed using the TOPAS software (Bruker AXS, Karlsruhe, Germany).

The petrographic characterization was performed on selected samples according to the EN 12407 standard [47]. The equipment used was a Carl Zeiss "Jenapol-U" polarized light optical microscope (POM) equipped with a digital camera (Nikon D7000) and the sections were half stained with alizarin to distinguish calcite from dolomite.

### 2.2. Calcination and study of the obtained quicklimes

Raw materials selected on the basis of their CI were ground into powder and calcined in graphite crucibles (109 × 95 × 61 $mm^3$) in a Hobersal JM22/16 kiln. Each crucible was filled with 50–60 g of sample to prevent high concentrations of $CO_2$ which could inhibit the formation of calcium oxide. Based on preliminary experimental tests undertaken on one of the samples, a calcination temperature of 1100 °C was selected, in agreement with Válek et al. [7]. The calcination conditions were as follows: heating ramp from 25 to 1100 °C of 2.5 h; gradient of 7.26 °C/min; dwell time at the maximum temperature of 2 h; cooling stage in the kiln (from 1100 to 25 °C) of 24 h. In total, the calcination process of each raw material took 28–29 h. Once taken out of the kiln, calcined samples were qualitatively analysed by means of XRD, in order to control the calcination process, and were subsequently preserved in closed Eppendorf's tubes and then placed in sealed plastic bags, to prevent reaction with $H_2O$ and $CO_2$ from the environment during storage. The Eppendorf's tubes were only opened for the analysis of the calcined samples by QPA, according to the quantitative method described above. The whole process of the XRD analysis, including sample preparation and measurement, took around 10 h, time during which the quicklimes were exposed to the laboratory conditions (RH = 60%; $T$ = 20 °C).

High-resolution field emission scanning electron microscope (HR-ESEM, FEI model Quanta 400) with EDS microanalysis (Bruker xFlash 6/30 detector) were also used on carbon-coated samples to observe the morphological and textural characteristics of the crystalline and amorphous phases developed in the quicklimes.

### 2.3. Slaking and study of the obtained NHLs

Slaking was undertaken by spreading each lime on a 2 × 30 × 40 $cm^3$ sized tray and spraying water in a 1:1 ratio of calcium oxide:water (amount calculated on the basis of the XRF data). The temperature rise caused by the exothermic reaction (due to transformation of CaO into Ca$(OH)_2$), was controlled by inserting a temperature sensor into the lime powder. The lime remained in the form of powder during the whole slaking process.

The evolution of quicklime to slaked lime was qualitatively monitored by X-ray diffraction at different time intervals: immediately after slaking and after 3, 5 and 7 days. Once stabilized, slaked samples were kept sealed in order to prevent further hydration and carbonation and were studied by means of XRD and QPAs.

## 3. Results and discussion

### 3.1. Study and selection of the raw materials

Raw materials from *Sierra Elvira* present the greatest compositional variability ($SiO_2$ = 4.34–76.87%, $Al_2O_3$ = 0.92–14.74%, $Fe_2O_3$ = 6.91–43%, CaO = 3.89–51.90%, MgO = 0.31–3.31%, Supplementary material 1). This is related to the fact that some of the limestone outcrops are more quartzitic and others more clayey or marly [40,43]. Samples from *Montefrío* have a lower content in reactive oxides ($SiO_2$ = 2.99–20.10%, $Al_2O_3$ = 0.49–2.49%, $Fe_2O_3$ = 0.31–0.92%, Supplementary material 1) and less dispersed values of calcium and magnesium oxides (CaO = 40.93–52.64%; MgO = 0.38–0.74%, Supplementary material 1). *Calicasas* is the area with the lowest amount of reactive oxides ($SiO_2$ = 0.65–10.34%; $Al_2O_3$ = 0.25–2.64%; $Fe_2O_3$ = 0.09–0.79%, Supplementary material 1) and the highest content in CaO and MgO (CaO = 46.47–53.60%; MgO = 0.73–1.69, Supplementary material 1). The mineralogy of all raw materials consists of calcite and quartz with similar percentages of clays (mainly illite), sometimes with plagioclase or feldspars and with dolomite and ilmenite as minor phases.

**Table 1**
Mineralogical composition (estimated standard deviations are reported in brackets), chemical composition of the main reactive oxides, and CI values of the 10 selected raw materials.

| Group | Sample | Mineralogical composition (wt%) | | | | | | | | Chemical composition (%) | | | | | |
|---|---|---|---|---|---|---|---|---|---|---|---|---|---|---|---|
| | | Calcite | Dolomite | Quartz | Plagioclase | K-feldspar | Illite | Kaolinite | Ilmenite | Amorphous | $SiO_2$ | $Al_2O_3$ | $Fe_2O_3$ | Total ($SiO_2 + Al_2O_3 + Fe_2O_3$) | MgO | CaO | CI |
| | | 76.50 | 0.19 | 1.48 (0.00) | 0.20 (0.00) | 0.00 | 2.93 | 0.00 | 0.41 | 18.30 (0.33) | 7.69 | 1.24 | 0.41 | 9.34 | 0.40 | 49.83 | 0.46 |
| | CA04 | (0.24) | (0.00) | | | (0.00) | (0.01) | (0.00) | (0.00) | | | | | | | | |
| | | 77.80 | 0.15 | 4.06 (0.01) | 0.00 (0.00) | 0.53 | 2.67 | 0.00 | 0.36 | 14.43 (0.39) | 5.65 | 2.20 | 0.69 | 8.54 | 0.73 | 49.76 | 0.37 |
| NHL2 | MF03 | (0.27) | (0.00) | | | (0.00) | (0.01) | (0.00) | (0.00) | | | | | | | | |
| | | 75.56 | 0.26 | 4.83 (0.02) | 0.30 (0.00) | 0.00 | 2.76 | 0.00 | 0.38 | 15.92 (0.35) | 8.30 | 1.58 | 0.67 | 10.55 | 0.77 | 48.40 | 0.51 |
| | SE27 | (0.24) | (0.00) | | | (0.00) | (0.01) | (0.00) | (0.00) | | | | | | | | |
| | | 70.38 | 0.37 | 4.71 (0.02) | 0.64 (0.00) | 0.26 | 3.83 | 1.00 | 0.42 | 18.40 (0.39) | 9.79 | 2.35 | 1.33 | 13.47 | 1.03 | 46.36 | 0.65 |
| NHL3.5 | SE10 | (0.26) | (0.00) | | | (0.00) | (0.01) | (0.00) | (0.00) | | | | | | | | |
| | | 64.24 | 0.32 | 5.81 (0.02) | 0.75 (0.00) | 0.00 | 6.08 | 1.96 | 0.32 | 20.51 (0.42) | 14.31 | 3.94 | 1.86 | 20.11 | 1.28 | 41.95 | 1.04 |
| | SE07 | (0.26) | (0.00) | | | (0.00) | (0.03) | (0.01) | (0.00) | | | | | | | | |
| | | 64.99 | 0.34 | 5.79 (0.03) | 1.21 (0.01) | 0.60 | 5.35 | 2.01 | 0.43 | 19.27 (0.46) | 12.82 | 3.48 | 1.80 | 18.10 | 1.20 | 43.51 | 0.91 |
| NHL5 | SE08 | (0.28) | (0.00) | | | (0.00) | (0.02) | (0.01) | (0.00) | | | | | | | | |
| | | 61.04 | 0.61 | 9.17 (0.04) | 0.00 (0.00) | 1.04 | 6.98 | 2.24 | 0.38 | 18.54 (0.45) | 16.90 | 3.55 | 1.74 | 22.19 | 1.28 | 41.58 | 1.21 |
| | SE13 | (0.26) | (0.00) | | | (0.00) | (0.03) | (0.01) | (0.00) | | | | | | | | |
| | | 65.96 | 0.00 | 9.26 (0.03) | 4.51 (0.01) | 0.00 | 1.00 | 0.00 | 0.40 | 18.87 (0.33) | 15.99 | 1.95 | 0.46 | 18.40 | 0.50 | 44.71 | 1.04 |
| | SE18 | (0.21) | (0.00) | | | (0.00) | (0.00) | (0.00) | (0.00) | | | | | | | | |
| Limit-NHB | | 55.38 | 0.18 | 18.35 | 3.55 (0.01) | 0.00 | 0.88 | 0.00 | 0.19 | 21.48 (0.34) | 27.95 | 3.59 | 1.12 | 32.66 | 0.65 | 35.99 | 2.25 |
| | SE23 | (0.18) | (0,00) | (0.06) | | (0.00) | (0.00) | (0.00) | (0.00) | | | | | | | | |
| | | 56.23 | 0.29 | 26.56 | 0.51 (0.00) | 0.00 | 2.20 | 0.00 | 0.38 | 13.82 (0.39) | 31.98 | 0.94 | 0.43 | 33.35 | 0.31 | 36.46 | 2.46 |
| | SE24 | (0.20) | (0.00) | (0.09) | | (0.00) | (0.01) | (0.00) | (0.00) | | | | | | | | |

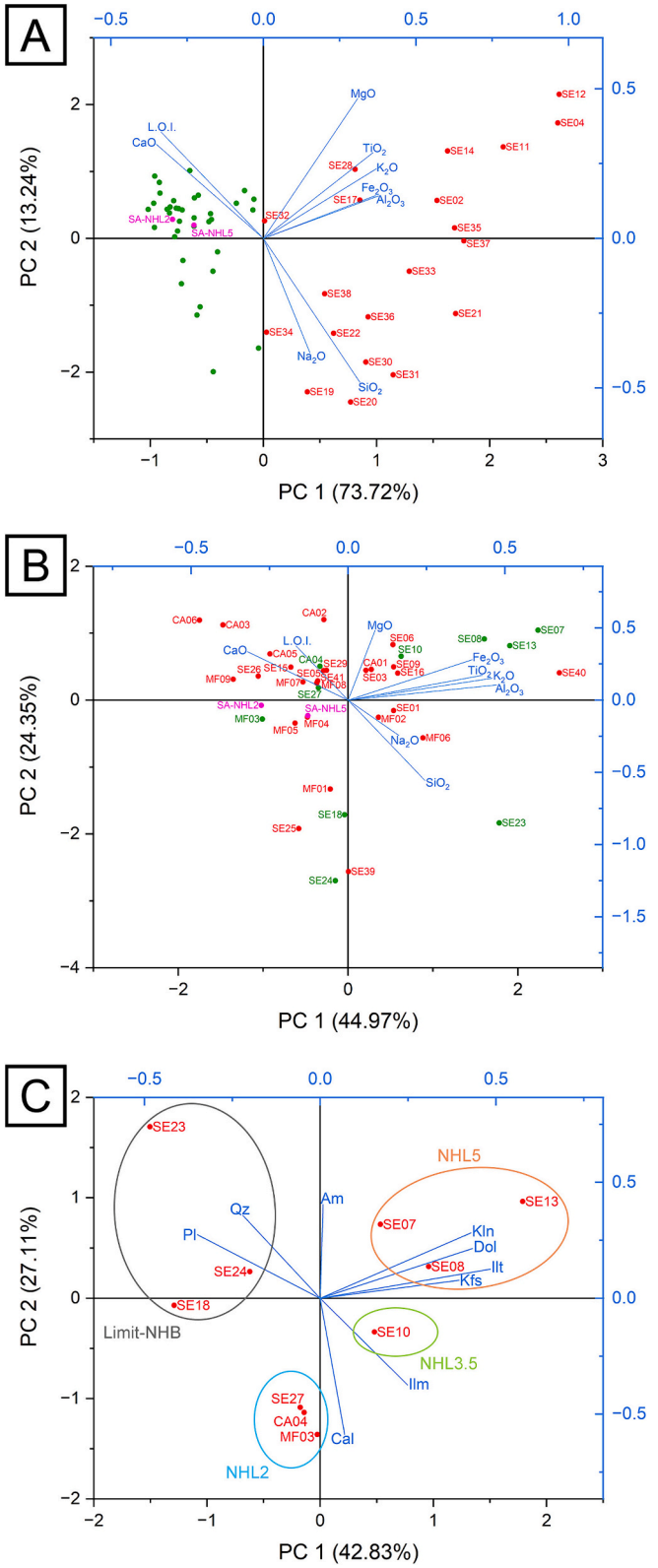


**Fig. 2.** A) Biplot of the principal component analysis (PCA) on the main oxides' composition of the full dataset of samples, measured by XRF. B) Biplot of the principal component analysis on the main oxides' composition of the set of samples selected after the first statistical treatment. C) Biplot of the principal component analysis on the quantitative mineralogical composition of the 10 selected raw materials. Abbreviations according to Warr [51]: Cal = calcite, Dol = dolomite, Ilm = ilmenite, Ilt = illite, Kfs = K-feldspar, Kln = kaolinite, Pl = plagioclase, Qz = quartz. Am = amorphous phases.

All samples also show a high amorphous component, likely ascribable to the paracrystalline fraction of clays.

There are certain discrepancies between the chemical results and the information on the geological maps, mainly because the outcropping rocks are not correctly described, as in the case of samples from *Montefrío*. These are defined as marls and marly limestones, and they have found to be, instead, siliceous limestones, according to the XRF data and the petrographic study.

Most samples are texturally classified according to Dunham [48] and Folk [49] as mudstones and dismicrites, with the exception of samples SE07 and SE08 (wackestones and biomicrites), SE10 (wackestone and dismicrite) and SE27 (packstone and biomicrite).

All samples display a clastic texture mud/supported matrix (<50% of clasts) with grains of quartz, phyllosilicates and K-feldspars (<100–200 μm) and different types of bio-clasts (ostracods, bryozoans, radiolarians, bivalves and crinoids) with dimensions between 200 μm and 1 mm. Most of the components are dispersed within a low porous micrite matrix, which as stated by Kozlovcev & Válek [33] is preferable to sparite for the manufacture of hydraulic binders due to its finer and well-distributed silicate particles. The quartz content observed under POM is lower than that detected by QPAs, due to the presence of microcrystalline quartz (flint), according to the description in the geological map.

Most of the samples from *Sierra Elvira* (SE) show CI values that are more in accordance with a natural cement than a natural hydraulic lime (Supplementary material 1), confirming that natural cement was effectively the main binder manufactured in the ancient factory located nearby [38,39]. Most samples from *Montefrío* (MF) and *Calicasas* (CA), instead, are unsuitable even for the production of feebly hydraulic limes (NHL2, CI = 0.3–0.5), as their CI values are too low.

Among the 56 raw materials studied, 10 samples were chosen for the manufacturing of NHL, according to their mineralogy, chemical composition, and CI values (Table 1). Selection and grouping were verified through principal component analyses (PCA [50] on XRF data (excluding MnO and $P_2O_5$, in proportions below 0.1%), using Origin Pro 2024 software (OriginLab Corporation) (Fig. 2A). In Fig. 2A, the first two components have been plotted, representing 86.97% of the total variance. Samples selected for further PCA are unlabelled and indicated in green, while those excluded are indicated in red. Reference commercial samples are indicated in magenta. After a first statistical treatment on the full dataset, samples too low in calcium oxide (characterized by positive principal components 1 (PC1) values, reported in red in Fig. 2A) were excluded, as they are not suitable for lime production. Then, a second PCA of the XRF data was performed on the remaining samples operating a further selection of 10 significant materials characterized by differentiated composition, as shown in Fig. 2B, where the first two components have been plotted, representing 69.32% of the total variance. Samples selected for this study are indicated in green, while reference commercial samples are indicated in magenta. On these samples, a further PCA was performed on their quantitative mineralogical profiles (Table 1), as shown in Fig. 2C, where the first two components have been plotted, representing 69.94% of the total variance.

According to the statistical analyses, three groups of raw materials were identified as suitable for the manufacture of feebly (NHL2), moderately (NHL3.5) and eminently (NHL5) natural hydraulic limes. A fourth group suitable for the production of natural hydraulic binders with higher hydraulicity (named Limit-NHB) were also considered.

The major differences among samples from each group are in the amount of reactive oxides and in the CI values, following the CI range detailed in literature: 0.3–0.5 for NHL2, 0.5–0.7 for NHL3.5, 0.7–1.1 for NHL5 and 1.1–1.7 for natural cements.

Samples for NHL2 production (CA04, MF03 and SE27) are positively correlated with high amounts of calcite (around 75% according to QPAs) and low aluminium and iron contents ($Al_2O_3$ = 1.24–2.20%, $Fe_2O_3$ = 0.41–0.69%, Table 1).

Group with samples SE07, SE08 and SE13, suitable for NHL5

**Table 2**
Mineralogical composition (estimated standard deviations are reported in brackets) of the 10 obtained quicklimes.

| Group | Sample | Mineralogical composition (wt%) | | | | | | | | | | | | | |
|---|---|---|---|---|---|---|---|---|---|---|---|---|---|---|---|
| | | Calcite | Lime | Periclase | Portlandite disordered | $C_2S$ | $C_3S$ | $C_3A$ | $C_4AF$ | Gehlenite | Wollastonite-2 M | Bredigite | Hydrogarnet | Ca-AFm | Quartz | Cristobalite | Amorphous |
| NHL2 | CA04 | 12.84 (0.07) | 14.06 (0.07) | 1.07 (0.01) | 37.73 (0.20) | 17.31 (0.09) | 0.28 (0.00) | 5.06 (0.03) | 0.76 (0.00) | 0.00 (0.00) | 0.00 (0.00) | 0.00 (0.00) | 0.00 (0.00) | 0.00 (0.00) | 0.08 (0.00) | 0.00 (0.00) | 10.81 (0.59) |
| | MF03 | 18.56 (0.09) | 23.87 (0.12) | 0.00 (0.00) | 4.83 (0.02) | 29.06 (0.14) | 0.60 (0.00) | 3.44 (0.02) | 0.44 (0.00) | 0.00 (0.00) | 0.00 (0.00) | 0.00 (0.00) | 0.00 (0.00) | 0.00 (0.00) | 0.00 (0.00) | 0.00 (0.00) | 19.20 (0.51) |
| | SE27 | 19.86 (0.09) | 15.36 (0.07) | 1.52 (0.01) | 19.92 (0.09) | 24.41 (0.11) | 0.00 (0.00) | 2.71 (0.01) | 0.85 (0.00) | 0.00 (0.00) | 0.00 (0.00) | 0.00 (0.00) | 0.00 (0.00) | 0.00 (0.00) | 0.00 (0.00) | 0.00 (0.00) | 15.37 (0.52) |
| NHL3.5 | SE10 | 20.26 (0.09) | 13.98 (0.06) | 1.35 (0.01) | 3.65 (0.02) | 31.01 (0.14) | 0.56 (0.00) | 3.25 (0.02) | 6.41 (0.03) | 0.00 (0.00) | 0.00 (0.00) | 0.00 (0.00) | 0.00 (0.00) | 0.00 (0.00) | 0.00 (0.00) | 0.00 (0.00) | 19.53 (0.48) |
| | SE07 | 2.94 (0.02) | 1.31 (0.01) | 1.50 (0.01) | 3.36 (0.02) | 51.04 (0.27) | 0.74 (0.00) | 1.11 (0.01) | 2.56 (0.01) | 1.99 (0.01) | 0.00 (0.00) | 5.27 (0.03) | 2.76 (0.02) | 2.16 (0.01) | 0.00 (0.00) | 0.00 (0.00) | 23.25 (0.54) |
| NHL5 | SE08 | 12.18 (0.06) | 3.34 (0.02) | 1.35 (0.01) | 4.91 (0.02) | 39.94 (0.20) | 1.71 (0.01) | 1.46 (0.01) | 5.08 (0.03) | 0.00 (0.00) | 0.00 (0.00) | 2.90 (0.01) | 2.30 (0.01) | 2.39 (0.01) | 0.00 (0.00) | 0.00 (0.00) | 22.44 (0.51) |
| | SE13 | 3.15 (0.02) | 2.03 (0.01) | 1.57 (0.01) | 2.88 (0.01) | 53.29 (0.26) | 0.73 (0.00) | 0.46 (0.00) | 7.06 (0.04) | 2.08 (0.01) | 0.00 (0.00) | 6.86 (0.03) | 0.00 (0.00) | 0.00 (0.00) | 0.00 (0.00) | 0.00 (0.00) | 19.88 (0.52) |
| | SE18 | 10.44 (0.05) | 4.76 (0.02) | 0.00 (0.00) | 13.55 (0.06) | 41.55 (0.19) | 0.27 (0.00) | 1.53 (0.01) | 1.69 (0.01) | 0.00 (0.00) | 0.00 (0.00) | 0.00 (0.00) | 0.00 (0.00) | 0.00 (0.00) | 0.00 (0.00) | 0.00 (0.00) | 26.22 (0.46) |
| Limit-NHB | SE23 | 0.00 (0.00) | 0.00 (0.00) | 0.00 (0.00) | 0.00 (0.00) | 25.34 (0.15) | 0.75 (0.00) | 0.00 (0.00) | 0.00 (0.00) | 20.85 (0.12) | 31.75 (0.18) | 0.00 (0.00) | 0.00 (0.00) | 0.00 (0.00) | 0.85 (0.01) | 0.00 (0.00) | 20.46 (0.61) |
| | SE24 | 0.00 (0.00) | 0.00 (0.00) | 0.00 (0.00) | 0.40 (0.00) | 44.36 (0.21) | 0.77 (0.00) | 0.00 (0.00) | 0.00 (0.00) | 6.93 (0.03) | 19.94 (0.10) | 3.53 (0.02) | 0.00 (0.00) | 0.00 (0.00) | 10.16 (0.05) | 1.92 (0.01) | 12.00 (0.55) |

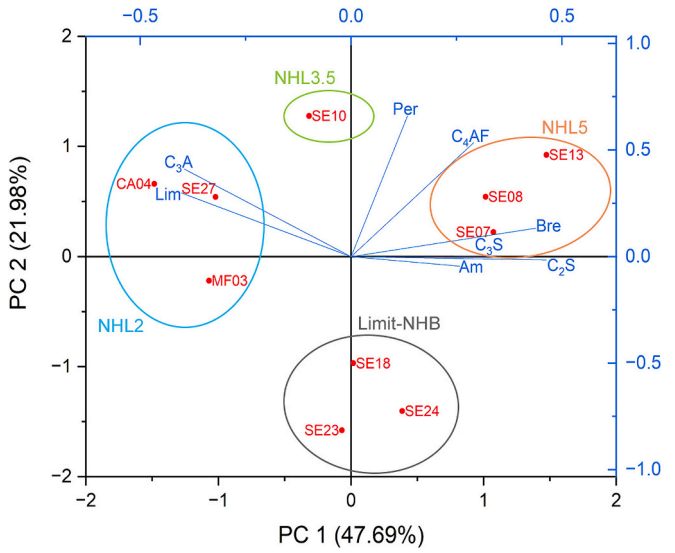


**Fig. 3.** Biplot of the principal component analysis on the quantitative mineralogical composition of the 10 selected quicklimes. Abbreviations: Am = amorphous phases, Bre = bredigite, $C_2S$ = larnite, $C_3S$ = hatrurite, $C_3A$ = celite, $C_4AF$ = brownmillerite, Lim = calcium oxide, Per = periclase.

production, are positively correlated with the highest percentages of clay minerals (around 3%) and high aluminium and iron contents ($Al_2O_3$ = 3.48–3.94%, $Fe_2O_3$ = 1.74–1.86%, Table 1).

The only sample suitable for NHL3.5 production (SE10) is in-between these two groups according to its chemical and mineralogical composition.

Samples SE18, SE23 and SE24, rich in silica and positively correlated with quartz and plagioclase according to PCA (Fig. 2C), do not fit in the established ranges of CI. Indeed, SE18 shows a CI value that is in the upper limit of NHL5, whilst SE23 and SE24 show CI values that exceed those established for natural cement. However, to follow the same criterion for all raw materials, according to the statistical analysis these three samples have been included in the same group, named Limit-NHBs. It should be noted that although all the samples show microcrystalline quartz and feldspars *s.l.* according to POM, samples belonging to Limit-NHB group have the highest contents of these mineral phases.

### 3.2. Study of the quicklimes

Table 2 shows the mineralogical composition of the 10 selected samples after calcination and storage in sealed Eppendorf's tubes and plastic bags. It can be seen that the highest lime contents (CaO) are found in samples belonging to NHL2 and NHL3.5 groups, while different kinds of hydraulic phases predominate in samples of the NHL5 and Limit-NHB group. These phases form after combination of reactive silica with calcium, iron and aluminium and magnesium, as detailed below.

Dicalcium silicate ($C_2S$), also known as larnite or *belite*, is predominant in all quicklimes (Table 2), in accordance with its enhanced formation at temperatures around 1100 °C [21,30]. Tricalcium silicate ($C_3S$), known as hatrurite or *alite*, is also present in most of the samples. Despite the formation of $C_3S$ is not expected in feebly hydraulic limes (NHL2), its presence might be justified for the existence of "*hot spots*" in the kiln [5,19].

Other mineral phases that have been found but are not so common in NHLs are brownmillerite ($C_4AF$, $Ca_2(Al,Fe)_2O_5$) and tricalcium aluminate ($C_3A$), known respectively as *felite* (or *ferrite*) and *celite*. Felite is an aluminium and iron-rich phase formed at temperatures above 1100 °C that, if in appropriate amounts, can promote sintering and reduce the calcination temperature [52], while celite is a tricalcium aluminate that

**Table 3**
Mineralogical composition (estimated standard deviations are reported in brackets) of the 10 obtained slaked limes.

| Group | Sample | Mineralogical composition (wt%) | | | | | | | | | | | | | | | |
|---|---|---|---|---|---|---|---|---|---|---|---|---|---|---|---|---|---|
| | | Calcite | Aragonite | Periclase | Portlandite | Portlandite disordered | C2S | C3S | C3A | C4AF | Gehlenite | Wollastonite-2 M | Bredigite | Hydrogarnet | Ca-AFm | Ca-AFm disordered | Quartz | Cristobalite | Amorphous |
| NHL2 | CA04 | 19.97 (0.14) | 0.00 (0.00) | 0.00 (0.00) | 11.87 (0.08) | 43.66 (0.30) | 7.53 (0.05) | 0.47 (0.00) | 0.39 (0.00) | 0.68 (0.00) | 0.00 (0.00) | 0.00 (0.00) | 0.00 (0.00) | 8.20 (0.06) | 0.21 (0.00) | 1.07 (0.01) | 0.00 (0.00) | 0.00 (0.00) | 5.96 (0.83) |
| | MF03 | 32.98 (0.19) | 0.00 (0.00) | 0.00 (0.00) | 11.38 (0.07) | 13.82 (0.08) | 11.93 (0.07) | 0.37 (0.00) | 0.00 (0.00) | 0.00 (0.00) | 0.00 (0.00) | 0.00 (0.00) | 0.00 (0.00) | 0.00 (0.00) | 7.77 (0.05) | 0.00 (0.00) | 0.11 (0.00) | 0.00 (0.00) | 21.64 (0.60) |
| | SE27 | 19.70 (0.12) | 0.00 (0.00) | 0.00 (0.00) | 5.12 (0.03) | 26.14 (0.16) | 10.11 (0.06) | 0.00 (0.00) | 0.00 (0.00) | 0.00 (0.00) | 0.00 (0.00) | 0.00 (0.00) | 0.00 (0.00) | 0.00 (0.00) | 2.68 (0.02) | 4.86 (0.03) | 0.32 (0.00) | 0.00 (0.00) | 31.08 (0.57) |
| NHL3.5 | SE10 | 18.17 (0.12) | 7.57 (0.05) | 0.54 (0.00) | 5.77 (0.04) | 10.14 (0.07) | 13.38 (0.09) | 0.00 (0.00) | 0.13 (0.00) | 0.38 (0.00) | 0.00 (0.00) | 0.00 (0.00) | 0.00 (0.00) | 2.86 (0.02) | 5.02 (0.03) | 3.56 (0.02) | 0.00 (0.00) | 0.00 (0.00) | 32.47 (0.60) |
| | SE07 | 8.79 (0.14) | 0.00 (0.00) | 0.82 (0.01) | 1.26 (0.02) | 0.81 (0.01) | 25.92 (0.40) | 0.59 (0.01) | 0.00 (0.00) | 0.28 (0.00) | 0.58 (0.01) | 0.00 (0.00) | 2.34 (0.04) | 7.66 (0.12) | 8.13 (0.13) | 5.51 (0.09) | 0.00 (0.00) | 0.00 (0.00) | 37.30 (0.14) |
| NHL5 | SE08 | 11.32 (0.08) | 0.00 (0.00) | 0.00 (0.00) | 0.73 (0.01) | 6.12 (0.04) | 22.09 (0.15) | 0.72 (0.00) | 0.07 (0.00) | 0.70 (0.00) | 0.00 (0.00) | 0.00 (0.00) | 0.64 (0.00) | 4.41 (0.03) | 10.22 (0.07) | 7.03 (0.05) | 0.00 (0.00) | 0.00 (0.00) | 35.94 (0.60) |
| | SE13 | 2.92 (0.02) | 5.77 (0.04) | 0.70 (0.00) | 2.99 (0.02) | 0.00 (0.00) | 21.07 (0.13) | 0.39 (0.00) | 0.00 (0.00) | 0.16 (0.00) | 1.77 (0.01) | 0.00 (0.00) | 2.42 (0.02) | 8.41 (0.05) | 3.48 (0.02) | 4.01 (0.03) | 0.00 (0.00) | 0.00 (0.00) | 45.91 (0.50) |
| Limit-NHB* | SE18 | 15.72 (0.10) | 0.00 (0.00) | 0.00 (0.00) | 10.05 (0.07) | 5.61 (0.04) | 26.10 (0.17) | 0.43 (0.00) | 0.00 (0.00) | 0.20 (0.00) | 0.00 (0.00) | 0.00 (0.00) | 0.00 (0.00) | 0.00 (0.00) | 3.85 (0.03) | 4.78 (0.03) | 0.00 (0.00) | 0.00 (0.00) | 33.27 (0.60) |
| | SE24 | 0.00 (0.00) | 0.00 (0.00) | 0.00 (0.00) | 0.34 (0.00) | 0.00 (0.00) | 32.45 (0.16) | 1.56 (0.01) | 0.00 (0.00) | 0.00 (0.00) | 6.87 (0.03) | 19.59 (0.10) | 1.92 (0.01) | 0.00 (0.00) | 0.00 (0.00) | 0.00 (0.00) | 8.61 (0.04) | 2.01 (0.01) | 26.64 (0.48) |

* The mineralogical profile of sample SE23 has not been reported since the amount of available material was too low for a reliable quantitative refinement.

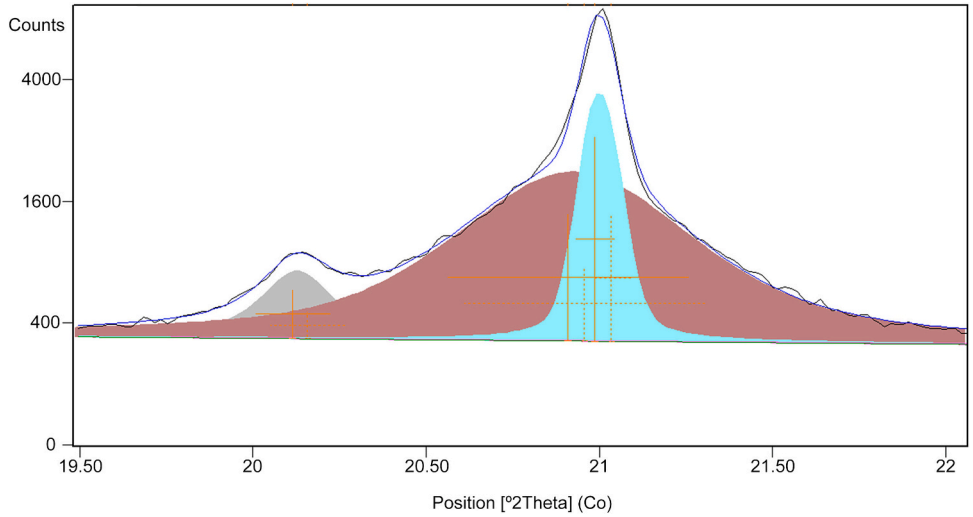


**Fig. 4.** XRPD pattern of sample CA04 after slaking, detail of the angular range including the diffraction reflex of portlandite's (001) basal plane (highlighted in maroon and cyan). The smaller peak (highlighted in grey) is related to the diffraction reflex of hydrogarnet's (211) plane. (For interpretation of the references to colour in this figure legend, the reader is referred to the web version of this article.)

can be present from 850 °C upwards [53]. Both are minor hydraulic phases frequently found both in laboratory-made NHLs and in some commercial varieties, when their raw materials have aluminium and iron contents of 1.23–4.02% and 0.43–1.50%, respectively [13,30,54,55].

Gehlenite ($Ca_2Al(SiAl)O_7$, $C_2AS$) and bredigite ($Ca_7Mg(SiO_4)_4$) are present only in some of the samples from NHL5 and Limit-NHB groups. Gehlenite is a calcium aluminium silico-aluminate that is formed at temperatures below 1200 °C [5]. In this study, it only formed in silica-rich samples (>14.30% of $SiO_2$) with $Al_2O_3$ and $Fe_2O_3$ contents between 0.94 and 3.94% and 0.43 and 1.86%, respectively. Gehlenite is considered, together with larnite, the main mineral phase of NHLs [5], and it has been detected in NHLs produced in other research studies [7,32,33], sometimes associated with åkermanite ($Ca_2Mg(Si_2O_7)$), a magnesium-rich non-hydraulic phase, forming a solid solution series in which magnesium is gradually replaced by aluminium [56]. In this study, although the presence of åkermanite, which can also be produced from wollastonite in MgO-rich systems, has not been detected [57], significant percentages of bredigite ($Ca_7Mg(SiO_4)_4$) have been found, mainly in association with gehlenite.

Bredigite is a high temperature mineral phase, generally considered non-hydraulic or of very slow hydration [58]. It has been found as a constituent of some slags [59], associated with the decomposition sequence bredigite-gehlenite-diaspore [60]. This phase is also found in cement clinkers [61,62], and there is much controversy about its mineral paragenesis, as several authors consider it as polymorph of larnite [59,63,64] while others associate it with gehlenite and spurrite ($Ca5(SiO_4)2CO_3$), a stable carbonate under conditions of high $CO_2$ concentrations and sufficient calcium silicate content [65].

The reactive silica that generated the above-mentioned hydraulic phases did not originate only from the clay fraction of the raw materials, but also from the microcrystalline quartz previously considered non-reactive. In sample SE24, quartz is partially transformed into its high-temperature polymorph cristobalite, whilst only in samples SE23 and SE24, those with the highest quartz content (>18%), belonging to the Limit-NHB group, wollastonite ($CaSiO_3$) was formed. This mineral has been previously detected in NHLs, and it is considered a non-hydraulic phase [7].

Furthermore, in some of the NHL5 samples, crystalline Ca-AFm phases belonging to the family of hydrated calcium aluminates (based on the hydrocalumite-type structure $4CaO\text{-}Al_2O_3\text{–}13\text{-}19H_2O$ [66]) are found. In the refinement procedure, these phases are best fitted with the structure of calcium monocarboaluminate (CAĈH [67]), a hydraulic mineral phase detectable in well hydrated pastes [68], and also frequently found in ancient materials with pozzolanic activity [69–71]. Although not all AFm phases are stable, several of them are persistent in pastes even at long curing times, and carbonate AFm phases are thermodynamically more stable than hydroxylated phases [66,67].

Periclase (MgO) has been detected in some samples, likely formed from Mg-containing mineral phases in the raw materials, such as magnesium carbonates (e.g. dolomite ($MgCa(CO_3)_2$) and/or phyllosilicates (e.g. illite $(K,H_3O)(Al,Mg,Fe)_2(Si,Al)_4O_{10}[(OH)_2,(H_2O)]$ [72]), both of them present in some of the raw materials studied. The fact that the content of MgO formed is not proportional to the Mg quantified in the raw material by XRF might be due to the heterogeneity of the rock itself. The presence of MgO in NHL may promote the formation of hydrated magnesium silicates (M-S-H [73]), which have been investigated recently for their binding capacity [74,75], as they seem to be responsible for the hydraulic features of Roman mortars [70], together with the better-known hydrated calcium silicates (C-S-H).

Samples belonging to the Limit-NHB group are characterized by distinctive mineralogical features. SE23 and SE24, whose CIs are higher than the upper limit established for natural cement, are characterized by the absence of lime formation after calcination, with the sole occurrence of silicate phases (mostly non-reactive) as a consequence of their high silica content. SE18, which has a CI value falling in the NHL5 group, is characterized by the occurrence of other phases such as calcite, portlandite and hydrogarnet ($Ca_3Al_2(O_4H_4)_3$), a mineralogical assemblage more similar to NHL5 than to natural cements. This finding confirms that the cementation index is a valid tool for the estimation of the degree of hydraulicity of the raw materials to be used for the production of natural hydraulic binders, in accordance with previous studies [7,13,29,30,33,45,76,77].

The presence of calcite in the quicklimes is something to be highlighted, considering that the calcination temperature is above the thermal decomposition range of this mineral phase [17] and the quicklimes had not been exposed to ambient $CO_2$, except for the time taken for sample preparation and XRD analysis (see Section 2.2), during which samples might have suffered carbonation. It is also possible that, due to the low power of the kiln extraction system, calcite have not been completely decomposed or post-carbonation reactions of quicklime in a $CO_2$-rich atmosphere have been produced [16,78]. This is not an uncommon process when obtaining NHL in laboratory muffles instead of industrial furnaces, because the released $CO_2$ reacts back with calcium

**Table 4**
Mineralogical composition (estimated standard deviations are reported in brackets) and chemical composition of the main reactive oxides of Saint Astier's NHL2 and NHL5 commercial limes.

| Sample | Mineralogical composition (wt%) | | | | | | | Chemical composition (%) | | | | | |
|---|---|---|---|---|---|---|---|---|---|---|---|---|---|
| | Calcite | Portlandite | Portlandite disordered | C2S | C3S | C3A | Quartz | Amorphous | $SiO_2$ | $Al_2O_3$ | $Fe_2O_3$ | Total ($SiO_2 + Al_2O_3 + Fe_2O_3$) | MgO | CaO | Cl |
| SA-NHL2 | 24.42 (0.19) | 31.10 (0.24) | 11.74 (0.09) | 13.44 (0.11) | 1.59 (0.01) | 1.80 (0.01) | 2.64 (0.02) | 13.27 (0.88) | 9.05 | 1.24 | 0.52 | 10.81 | 0.87 | 64.68 | 0.41 |
| SA-NHL5 | 31.27 (0.21) | 6.38 (0.04) | 9.29 (0.06) | 15.18 (0.10) | 8.90 (0.06) | 2.64 (0.02) | 2.98 (0.02) | 23.37 (0.68) | 14.26 | 1.73 | 0.65 | 16.64 | 1.12 | 60.28 | 0.68 |

oxide [16,78] or even with other reactive oxides to form carbonates. As an example, Kozlovcev & Přikryl [30] have obtained spurrite ($Ca_5(SiO_4)_2CO_3$), a carbonated calcium silicate.

Special attention must be given to the identification of a fraction of disordered portlandite in the quicklimes (Table 2), characterized by mean crystallite sizes lower than 20 nm. It is interesting to notice that portlandite was not detected in the quicklimes qualitatively analysed right after calcination (see Supplementary materials 2, 3, 4 and 5), but it was present in the quicklimes analysed by QPA (Table 2). These data, although apparently discordant, are showing that during samples preparation and QPA analysis (process that lasts around 10 h in contrast to the 15 min duration of qualitative XRD analyses) quicklimes undergo a partial slaking, due to simple exposure to the laboratory conditions (RH = 60%; $T$ = 20 °C). This result is remarkable for two reasons: i) it indicates that hydration of CaO into $Ca(OH)_2$ occurs without the need of adding water to the quicklime, and ii) portlandite formed under these conditions shows a disordered crystalline structure, potentially leading to a higher reactivity towards carbonation.

In a similar way, in the quicklimes analysed by QPA, the transformation of $C_3A$ and $C_4AF$ into hydrogarnet [79] has been observed, suggesting that also a partial hydration process occurs during sample handling.

Finally, the amorphous fraction found in all samples is to be ascribed to paracrystalline/amorphous components of the reactive phases, although a partial correlation to the occurrence of hydrated hydraulic phases (mainly C-S-H) cannot be excluded, given the aforementioned presence of hydrated phases such as hydrogarnet. It must be highlighted that, if calcium silicate hydrates are formed, is also likely that part of the disordered portlandite comes from the hydration reaction between the $CaO\text{-}SiO_2$ system and water that leads to the release of C-S-H and $Ca(OH)_2$ [68].

Fig. 3 shows the results of the PCA performed on the quantitative mineralogical profiles of the quicklimes (Table 2), after excluding the non-reactive (calcite, quartz, cristobalite, wollastonite and gehlenite) and hydrated (portlandite, AFm and hydrogarnet) phases. In this figure, the first two components have been plotted, representing 69.67% of the total variance.

Samples cluster in the same way as in the raw materials, thus indicating that the chemical and mineralogical composition of the raw materials is directly related to the mineralogy they develop after calcination.

More in detail, samples of the NHL2 group, whose raw materials had the highest calcite contents and the lowest amounts of iron and aluminium oxides, show a predominance of crystalline calcium oxide. The sample defined for the manufacture of NHL3.5 still shows intermediate values between NHL2 and NHL5, and samples in the NHL5 group show, as expected, a high content in hydraulic phases. Finally, samples from Limit-NHB group are still grouped, although only SE18 was the only one to develop quicklime.

### 3.3. Study of the slaking process

During the slaking process, the highest temperatures recorded were 96 °C in sample CA04 (NHL2 group), followed by samples SE10 (NHL3.5 group) and SE13 (NHL5), both with a maximum temperature around 75 °C. This is in agreement with the initial calcite and calcium oxide content of their respective raw materials (Table 1). The exothermic reaction of these samples occurred immediately after the water addition and with an associated volume increase.

In remaining samples moderate exothermic reactions occurred with temperatures reaching an average of 40–45 °C, except for samples SE07 (from NHL5 group), SE23 and SE24 (from Limit-NHBs), only reaching 28 °C. These least reactive samples showed a temperature rise only after 10 min, and hardly changed their volume. Indeed, null to little lime (CaO) was present in these binders after calcination (Table 2), and therefore portlandite was not formed, also due to the high content of

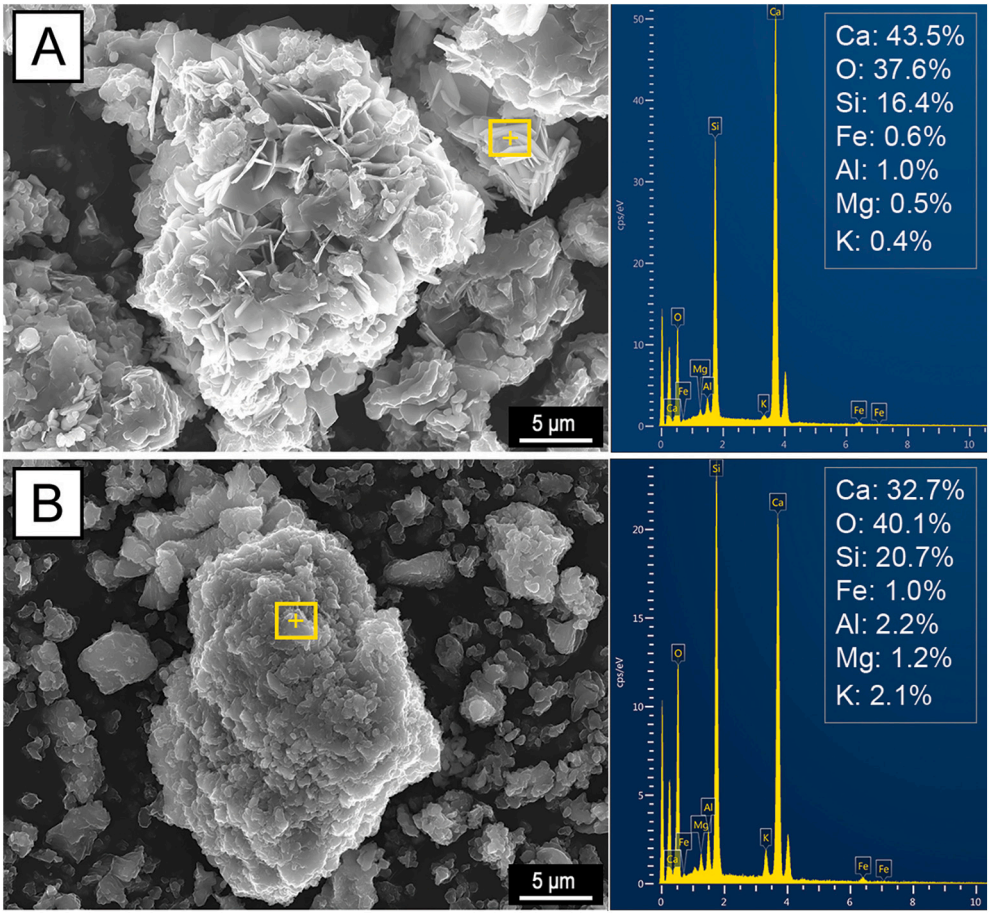


**Fig. 5.** HR-ESEM images of: A) one of the slaked limes from NHL5 group and B) Saint Astier's NHL5, with their respective EDS spectra and relative percentages of each element identified. The analysed area is marked with a yellow rectangle. (For interpretation of the references to colour in this figure legend, the reader is referred to the web version of this article.)

reactive oxides ($Al_2O_3$, $SiO_2$ and/or $Fe_2O_3$) that hindered or reduced the free lime content.

After slaking, all samples showed a total consumption of calcium oxide, with a clear occurrence of two populations of portlandite, a crystalline and a disordered one, characterized by significantly different mean crystallite sizes (higher than 100 nm and lower than 20 nm, respectively (Table 3)), as indicated by the complex articulation of the diffraction reflexes with two convoluted pseudo-gaussian distributions (Fig. 4): the larger one (highlighted in maroon) is related to a disordered portlandite fraction, while the sharper one (highlighted in cyan) is ascribable to a highly crystalline component.

Considering that only disordered portlandite was found in the quicklimes analysed by QPA, it is evident that standard slaking has given place to a more crystalline portlandite structure. This fact is worth to be highlighted, as it will influence the reactivity of the aerial part of NHL towards the carbonation process.

The influence of the air exposure of quicklime on the hydration of calcium oxide was already highlighted by Potgieter et al. [16], who affirmed that air slaking, among other factors, significantly reduces the slaking capacity of air lime. However, it must be noticed that in Potgieter et al.'s study [16], limes were subjected to prolonged periods under humid atmospheric conditions, which promoted the appearance of an external layer of calcium hydrate and/or calcium carbonate on the surface of the quicklime particles that might have been hindered further carbonation of the lime, thus reducing its reactivity.

Furthermore, mineralogical analyses on the slaked samples highlight a significant decrease of all main hydraulic phases ($C_2S$, $C_3S$, $C_3A$ and $C_4AF$) with respect to their calcined counterparts, with a correspondent increase of hydrated calcium aluminates (hydrogarnet and Ca-AFm, the latter characterized by two populations, a disordered and a crystalline one, with differentiated mean crystal sizes). Such evidence is a strong indication of the hydration tendency of hydraulic phases during the slaking process, and this hypothesis is further corroborated by the relevant increase in amorphous phases, likely ascribable to para-crystalline fractions of hydrated compounds, in particular C-S-H, often characterized by the lack of long-range crystalline ordering [80].

Finally, the exposure of samples to $CO_2$ during slaking explains the partial carbonation of portlandite into calcite and aragonite, the latter polymorph probably formed due to the high temperatures reached during slaking.

### *3.4. Overall evaluation of the laboratory-manufactured NHLs and comparison with commercial NHLs*

Once in their final form, the laboratory-manufactured NHLs need to be evaluated according to the chemical requirements established by the European specifications [27], among them, the minimum content of free lime (expressed as $Ca(OH)_2$), which must be: ≥35% for NHL2, ≥25% for NHL3.5, and ≥ 15% for NHL5. This amount was calculated from the total content of portlandite (crystalline and disordered) of Table 3. In the first group, only sample CA04 gives a NHL2 that complies with the chemical requirements, as $Ca(OH)_2$ in this lime is 55.53%. In the other two limes belonging to the NHL2 group, the content of $Ca(OH)_2$ is slightly lower than 35%: 25.2% in MF03 and 31.26% in SE27. However, the high $CaCO_3$ content in these limes might explain a lower amount of $Ca(OH)_2$ than expected, as the latter could have suffered a partial

carbonation during sample handling. The same can be interpreted for sample SE10, giving a NHL3.5 with only 15.91% of $Ca(OH)_2$ but with >18% of calcite; and for sample SE08, giving a NHL5 with 6.85% of $Ca(OH)_2$ and 11.32% of calcite. Only two of the NHLs produced, SE07 and SE13, both from the NHL5 group according to the cementation index of the raw materials, do not comply with the minimum content of free lime, as even though the content of calcite is summed to that of portlandite, their sum does not reach the required 15% (the sum is 10.86% in SE07 and 5.91% in SE13). From the group of limit-NHB, sample SE18 contains 15.66% of $Ca(OH)_2$ (which could be even higher if we consider the additional 15.72% of calcite in this binder), factor that allows it to be placed in the NHL5 group, also considering the similar content in $C_2S$ of this sample compared to samples from the NHL5 group.

The chemical-mineralogical data of the NHLs obtained in this study were also compared with those of the NHL2 and NHL5 purchased from the French company Saint Astier (SA-NHLs). SA-NHLs (Table 4) are composed of calcite, portlandite, calcium silicates ($C_2S$ and $C_3S$) and calcium aluminates ($C_3A$), quartz and amorphous phases. As in slaked NHLs (Table 3), also SA-NHLs contain both ordered and disordered portlandite, suggesting that commercial NHLs from Saint Astier might also have undergone an air exposure period before slaking that led to the formation of a fraction of calcium hydroxide with low crystallinity.

A general difference among our samples and commercial NHLs is the high calcite content in the latter (24–31%), part of which might have formed due to carbonation during sample handling (as in the laboratory-manufactured NHLs). As industrial kilns have powerful extraction systems, this cannot be explained by the occurrence of re-carbonation reactions. Given that the calcination temperatures reached at the Saint Astier factory do not exceed 950 °C [81], it is more likely that low-T points were generated in the kiln, which would explain the presence of unburnt calcite in all SA-NHL, and the formation of the low temperature silica polymorph, tridymite, in SA-NHL5. Inhomogeneities in the operative temperatures of the industrial kiln would also support the higher $C_3S$ amounts (especially in SA-NHL5 sample) with respect to the experimental samples, likely related to the establishment of localized high-T points.

Other relevant differences between our experimental samples and the reference commercial products are related to the amount of hydrated calcium aluminates, since hydrogarnet content is systematically lower in the limes from Saint Astier, and AFm phases are absent. This evidence should not be related to a lower degree of hydration of the hydraulic phases during slaking, since amorphous content is relevant in both the commercial products, leading to hypothesise a significant occurrence of paracrystalline hydrated phases (mainly C-S-H) even in these NHLs. It should be instead related to the chemical composition of the raw materials employed in the Saint Astier production plant, characterized by lower alumina and ferrite content with respect to our experimental products (Table 4, Supplementary material 1), and thus less favourable for crystallization of calcium aluminoferrites during the firing process.

The mineralogical differences between laboratory-manufactured and commercial NHLs were greater when comparing limes from the NHL5 group. Our NHL5 contains periclase, brownmillerite ($C_4AF$), gehlenite and bredigite, not present in SA-NHL. These mineralogical differences might be justified considering the compositional differences of the raw materials used and/or differences in the manufacturing process (different calcination temperatures and dwell times).

To understand the effect of the calcination temperature in the development of mineral phases, calcination tests were carried out at different temperatures on only one of the 10 samples studied here (SE08), selected randomly. Calcination temperatures were: 950 °C, as it is the temperature used in Saint Astier factory [81]; 1100 °C, the most accepted calcination temperature according to Válek et al. [7] study; and 1250 °C, the upper limit before the triggering of relevant sintering processes [5]. Calcination tests were performed with heating ramps of about 7 °C/min and dwell times of 30 min in the kiln.

In agreement with previous studies by Válek et al. [7], the XRD analyses performed on the obtained quicklimes indicated that the higher the temperature, the higher the content of hydraulic phases, with a significant lowering of the calcite content (see Supplementary material 6).

Furthermore, spurrite was detected at all the calcination temperatures, as in Kozlovcev & Přikryl [30], confirming the theory of back-reactions in which the released $CO_2$ reacts with reactive oxides [78].

The sample used for the calcination tests showed also the occurrence of iron-bearing hydraulic phases (rankinite ($Ca_3Si_2O_7$, C3S2) and andradite ($Ca_3Fe_2(SiO_4)_3$)), which turned the colour of the obtained quicklime darker (mostly brownish, Supplementary material 6). Rankinite is a non-hydraulic phase, although it can enhance carbonation reaction at low water/solid ratios, leading to the formation of calcite/vaterite and polymerised silica gel [82]. Andradite is a garnet formed from the combination of Ca, Si and Fe oxides that can form in geopolymerisation processes when slags are used [72]. Iron-bearing mineral phases were not found in commercial SA-NHLs, suggesting that their formation is not favoured at 950 °C.

Through SEM-EDX analyses, it is possible to observe the morphology of laboratory and commercial NHLs and to confirm the elemental chemical composition of many of the mineral phases determined by XRD. It is worth highlighting the small size of the calcium silicates (<2 μm), mainly $C_2S$ according to the Ca/Si ratios (Fig. 5). A small particle size could trigger a higher reactivity of $C_2S$ towards water, due to a higher specific surface area, which would explain the presence of hydrated phases both in the stored quicklimes and in the slaked products. A fact that might not occur in all hydraulic binders, as is the case of Portland cement, where dicalcium silicate particles, characterized by average dimensions between 20 and 40 μm [53], undergo a very slow hydration process, which is the responsible for the late development of mechanical strength in this binder.

## 4. Conclusions

This study confirms that some of the investigated outcrops in the province of Granada (Andalusia, Spain) are suitable for the manufacture of natural hydraulic limes with different hydraulicity degrees.

The selected raw materials satisfied the required cementation indexes and reactive oxides contents for the development of hydraulic phases. The sources of silica were both clay minerals and microcrystalline quartz, confirming that not only clayey limestones but also siliceous ones are suitable for the manufacturing of NHLs.

Moreover, it should be noted that the heterogeneity of the outcrops (some more quartzitic, others more clayey and others more calcareous) might limit the extraction areas, making the selection of raw materials more complex from an industrial point of view.

This study confirms that the hydraulicity and reactivity of natural hydraulic limes strongly depend on the chemical-mineralogical composition and textural characteristics of the raw material and on the calcination conditions in the kiln.

Regarding the slaking process, it was found that NHL quicklimes (i.e. after calcination) undergo a natural slaking process through even short periods of air exposure, leading to the formation of a more disordered and potentially more reactive portlandite fraction compared to that formed during slaking by addition of water. Furthermore, it has been demonstrated that “passive slaking” by air exposure reduces the undesired reaction of some of the hydraulic phases, which have been found to suffer a partial hydration during standard slaking. Despite a partial reaction of the aluminoferritic phases into AFms and hydrogarnet seems to occur even under air exposure conditions, the hydration of dicalcium silicate ($C_2S$) can be reduced if standard slaking is not performed.

The limitations of this research study (i.e. the use of local raw materials does not enable to manufacture the same NHLs in other localities and/or geographic areas; and the heterogeneity of the rock outcrops and raw materials themselves might lead to different NHLs) are certainly overcome by the fact that it lays the basis for future research on NHL.

Further studies on the influence of different conditions of "passive" slaking of the quicklime (e.g. air exposure under different relative humidity values) on the reactivity of the final NHL are needed to define optimal manufacturing conditions. In particular, it is necessary to investigate if the disordered portlandite formed during air exposure is due to the hydration of CaO or is generated after reaction of $C_2S$ with water to form C-S-H and $Ca(OH)_2$.

Supplementary data to this article can be found online at https://doi.org/10.1016/j.cemconres.2024.107631.

## Funding

This work was supported by the State Research Agency (SRA) and the Ministry of Science and Innovation under the Research Project PID2020-119838RA-I00, the Regional Ministry of University Research and Innovation of the Junta de Andalucía and FEDER (*a way of making Europe*) B-RNM-188-UGR20, and the Junta de Andalucía Research Group RNM179.

## CRediT authorship contribution statement

**C. Parra-Fernández:** Writing – original draft, Methodology, Investigation, Formal analysis. **A. Arizzi:** Writing – review & editing, Visualization, Supervision, Project administration, Investigation, Funding acquisition, Data curation, Conceptualization. **M. Secco:** Writing – review & editing, Data curation. **G. Cultrone:** Writing – review & editing.

## Declaration of competing interest

The authors report there are no competing interests to declare.

## Data availability

Data will be made available on request.

### *Acknowledgements*

We thank Salvador Morales Ruano and Mª Gracia Bagur González for their assistance during sampling. We are also grateful to Nigel Walkington for his assistance in revising the manuscript.

### *Authors statement*

All the authors are aware of the submission of this revised version.

## References

[1] A.D. Cowper, Lime and Lime Mortars vol. 14, Donhead Publishing Ltd, Shaftesbury, 1927.
[2] S. Holmes, M. Wingate, Building with Lime: A Practical Introduction vols. 12-14, Intermediate Technology Publications Ltd, Warwickshire, 1997.
[3] G. Mertens, J.E. Lindqvist, D. Sommain, J. Elsen, Calcareous hydraulic binders from a historical perspective, in: Proceedings of the 1st Historic Mortars Conference: Characterization, Diagnosis, Conservation, Repair and Compatibility, HMC08, Lisbon, 2008, pp. 1–15.
[4] C. Figueiredo, M. Lawrence, R.J. Ball, Chemical and physical characterization of three NHL2 and the relationship with the mortar properties, in: L. Villegas, I. Lombillo, H. Blanco, Y. Boffill (Eds.), REHABEND Euro-American Congress: Construction Pathology, Rehabilitation Technology and Heritage Management (6th REHABEND Congress), Burgos, 2016, pp. 1–8. CODE: 2.2.17.
[5] K. Callebaut, J. Elsen, K. Van Balen, W. Viaene, Nineteenth century hydraulic restoration mortars in the Saint Michael's Church (Leuven, Belgium): natural hydraulic lime or cement? Cem. Concr. Res. 31 (3) (2001) 397–403, https://doi.org/10.1016/S0008-8846(00)00499-3.
[6] D.C. Hughes, D.B. Sugden, D. Jaglin, D. Mucha, Calcination of Roman cement: a pilot study using cement-s-tones from Whitby, Construct. Build Mater. 22 (7) (2008) 1446–1455, https://doi.org/10.1016/j.conbuildmat.2007.04.003.
[7] J. Válek, E. Van Halem, A. Viani, M. Pérez-Estébanez, R. Ševčík, P. Šašek, Determination of optimal burning temperature ranges for production of natural hydraulic limes, Construct. Build Mater. 66 (2014) 771–780, https://doi.org/10.1016/j.conbuildmat.2014.06.015.
[8] J. Válek, Lime technologies of historic buildings, preparation of specialised lime binders for conservation of historic buildings, in: Ústav Teoretické a Aplikované Mechaniky Akademie Věd České Republiky (ÚTAM AV ČR), Prague, 2015.
[9] J.A.H. Oates, Lime and Limestone: Chemistry and Technology, Production and Uses, Wiley-VCH, Weinheim, Germany, 1998.
[10] W. Gallala, M.E. Gaied, A. Tlili, M. Montacer, Factors influencing the reactivity of quicklime, Proceedings of the Institution of Civil Engineers-Construction Materials 161 (1) (2008) 25–30, https://doi.org/10.1680/coma.2008.161.1.25.
[11] D. Carran, J. Hughes, A. Leslie, C. Kennedy, The effect of calcination time upon the slaking properties of quicklime, in: J. Válek, J. Hughes, C.J.W.P. Groot (Eds.), Historic Mortars: Characterisation, Assessment and Repair, RILEM Bookseries, Springer, vol. 7, Dordrecht, Netherlands, 2012, pp. 283–295.
[12] G. Leontakianakos, I. Baziotis, E. Profitis, E. Chatzitheodoridis, S. Tsimas, Assessment of the quality of calcination of marbles from Thassos Island using Raman spectroscopy and X-Ray diffraction, Bull. Geol. Soc. Greece 47 (4) (2013) 2040–2049, https://doi.org/10.12681/bgsg.11088.
[13] G. Vola, P. Bresciani, E. Rodeghero, L. Sarandrea, G. Cruciani, Impact of rock fabric, thermal behavior, and carbonate decomposition kinetics on quicklime industrial production and slaking reactivity, J. Therm. Anal. Calorim. 136 (2019) 967–993, https://doi.org/10.1007/s10973-018-7769-7.
[14] EN 459–2, Building Lime: Test Methods, CEN, European Committee for Standardization, 2021.
[15] S.K. Afridi, M.B. Bhatty, A.S. Ahmed, M.T. Saeed, S. Ahmad, Experimental study of calcination-carbonation process for the production of precipitated calcium carbonate, J. Chem. Soc. Pak. 30 (4) (2008) 559–562.
[16] J.H. Potgieter, S.S. Potgieter, S.J. Moja, A. Mulaba-Bafubiandi, An empirical study of factors influencing lime slaking, Part I: production and storage conditions, Minerals Engineering 15 (3) (2002) 201–203, https://doi.org/10.1016/S0892-6875(02)00008-0.
[17] M. Földvári, Handbook of Thermogravimetric System of Minerals and its Use in Geological Practice, Occasional Papers of the Geological Institute of Hungary vol. 213, 2011. Budapest, Hungary.
[18] C. Mayo Corrochano, D. Sanz Arauz, J.I. Pineda Enebra, Metodología simplificada de identificación mediante MOP de las cales hidráulicas y los cementos naturales, in: J.I. Álvarez Galindo, J.M. Fernández Álvarez, I. Navarro Blasco, A. Durán Benito, R. Sirera Bejarano (Eds.), VI Jornadas FICAL Fórum Ibérico de la Cal "Tradición, versatilidad e innovación en la cal: un material de excelencia", Pamplona, 2018, pp. 188–199.
[19] A.F. Gualtieri, A. Viani, C. Montanari, Quantitative phase analysis of hydraulic limes using the Rietveld method, Cem. Concr. Res. 36 (2) (2006) 401–406, https://doi.org/10.1016/j.cemconres.2005.02.001.
[20] P. Livesey, Succeeding with hydraulic lime mortars, J. Archit. Conserv. 8 (2) (2002) 23–37, https://doi.org/10.1080/13556207.2002.10785317.
[21] G. Allen, Hydraulic Lime Mortar for Stone, Brick and Block Masonry, Donhead Publishing Ltd, Shaftesbury (UK), Shaftesbury, 2003.
[22] J. Lanas, J.L. Pérez Bernal, M.A. Bello, J.I. Álvarez Galindo, Mechanical properties of natural hydraulic lime-based mortars, Cem. Concr. Res. 34 (12) (2004) 2191–2201, https://doi.org/10.1016/j.cemconres.2004.02.005.
[23] M. Forsyth, in: M. Forsyth (Ed.), Materials & Skills for Historic Building Conservation, Blackwell, Oxford, 2008.
[24] A. El-Turki, R.J. Ball, S. Holmes, W.J. Allen, G.C. Allen, Environmental cycling and laboratory testing to evaluate the significance of moisture control for lime mortars, Construct. Build Mater. 24 (8) (2010) 1392–1397, https://doi.org/10.1016/j.conbuildmat.2010.01.019.
[25] A. Henry, J. Stewart, English Heritage, Practical Building Conservation. Mortars, Renders & Plasters, Ashgate, Farnham, 2012.
[26] G. Mertens, Characterisation of Historical Mortars and Mineralogical Study of the Physico-Chemical Reactions on the Pozzolan-Lime Binder Interface, PhD Thesis,, Catholic University of Leuven, 2009.
[27] EN 459–1. Building Lime - Part 1: Definitions, Specifications and Conformity Criteria, CEN, European Committee for Standardization, 2015.
[28] A. Moropoulou, A. Bakolas, E. Aggelakopoulou, The effects of limestone characteristics and calcination temperature to the reactivity of the quicklime, Cem. Concr. Res. 31 (4) (2001) 633–639, https://doi.org/10.1016/S0008-8846(00)00490-7.
[29] H. Böke, Ö. Çizer, B. İpekoğlu, E. Uğurlu, K. Şerifaki, G. Toprak, Characteristics of lime produced from limestone containing diatoms, Construct. Build Mater. 22 (5) (2008) 866–874, https://doi.org/10.1016/j.conbuildmat.2006.12.010.
[30] P. Kozlovcev, R. Přikryl, Devonian micritic limestones used in the historic production of Prague hydraulic lime ('pasta di Praga'): characterization of the raw material and experimental laboratory burning, Mater. Constr. 65 (319) (2015) 1–16, https://doi.org/10.3989/mc.2015.06314.
[31] G. Leontakianakos, I. Baziotis, A. Papandreou, D. Kanellopoulou, V. N. Stathopoulos, S. Tsimas, A comparative study of the physicochemical properties of Mg-rich and Ca-rich quicklimes and their effect on reactivity, Mater. Struct. 48 (2015) 3735–3753, https://doi.org/10.1617/s11527-014-0436-y.
[32] G. Vola, L. Sarandrea, G. Della Porta, A. Cavallo, F. Jadoul, G. Cruciani, The influence of petrography, mineralogy and chemistry on burnability and reactivity of quicklime produced in Twin Shaft Regenerative (TSR) kilns from Neoarchean limestone (Transvaal Supergroup, South Africa), Mineral. Petrol. 112 (2018) 555–576, https://doi.org/10.1007/s00710-017-0542-y.
[33] P. Kozlovcev, J. Válek, The micro-structural character of limestone and its influence on the formation of phases in calcined products: natural hydraulic limes and cements, Materials and Structures/Materiaux et Constructions 54 (217) (2021) 1–27, https://doi.org/10.1617/s11527-021-01814-7.

[34] K.W. Ray, F.C. Mathers, Effect of temperature and time of burning upon the properties of high-calcium lime, Ind. Eng. Chem. 20 (4) (1928) 415–419, https://doi.org/10.1021/ie50220a030.
[35] K.C. Ray, P.C. Sen, M.R.K. Rao, Studies on reactivity of lime, Trans. Indian Ceram. Soc. 42 (5) (1983) 115–119, https://doi.org/10.1080/0371750X.1983.10822646.
[36] M. Rodríguez Avila, Investigaciones analíticas sobre cales hidráulicas de la provincia de Granada, in: Congreso de la Asociación Española para el Progreso de la Ciencia, Sección 3ª Ciencias Físicoquímicas, Granada, 1912, pp. 19–32.
[37] R.S. Boynton, Chemistry and Technology of Lime and Limestone, second ed., John Wiley and Sons, Inc., New York, 1980.
[38] M.A. Rubio Gandía, M. Giménez Yanguas, J.M. Reyes Mesa, Patrimonio Industrial en Granada, Auskaria Mediterránea, Granada, 2003.
[39] J.A. Porta Igual, La Fábrica de cemento Portland artificial y cal hidráulica Nª Señora de los Dolores en Atarfe: estudio histórico y de producción, Trabajo Fin de Máster, Universidad de Granada, 2016.
[40] Instituto Geológico y Minero de España, Mapa geológico de España. Escala 1: 50.000. Hoja 1009/19–41. Granada. DL: M-30.451. https://info.igme.es/cartografiadigital/geologica/Magna50Hoja.aspx?Id=1009, 1988.
[41] Instituto Geológico y Minero de España, Mapa geológico de España. Escala 1: 50.000. Hoja 1008/18–41. Montefrío. DL: M-30.452. https://info.igme.es/cartografiadigital/geologica/Magna50Hoja.aspx?Id=1008, 1988.
[42] Instituto Geológico y Minero de España, Mapa geológico de España. Escala 1: 50.000. Hoja 990/18–40. Alcalá la Real. DL: M-10.720-1992. https://info.igme.es/cartografiadigital/geologica/Magna50Hoja.aspx?Id=990, 1992.
[43] S. Morales Ruano, A. Arizzi, G. Cultrone, C. Parra-Fernández, M.G., Bagur González, Geoquímica de niveles carbonatados de la provincia de Granada utilizables para la fabricación de cal hidráulica natural: datos preliminares, Macla: Revista de la Sociedad Española de Mineralogía. 26 (2022) 132–133.
[44] Geological Map of Spain ArcGis Web map at a scale of 1:50.000, 2015. https://ige.maps.arcgis.com/home/webmap/viewer.html?webmap=92d3a8e400b44daf911907d3d7c8c7e9. Last access: 01/07/2022.
[45] E.C. Eckel, Cement, Limes and Plasters: Their Materials, Manufacture and Properties, John Wiley and Sons, London, 1922.
[46] H. Rietveld, A refinement method for nuclear and magnetic structures, J. Appl. Cryst. 2 (1969) 65–71, https://doi.org/10.1107/S0021889869006558.
[47] EN 12407, Natural Stone Test Methods - Petrographic Examination, CEN, European Committee for Standardization, 2019.
[48] R.J. Dunham, Classification of carbonate rocks according to depositional texture, in: W.E. Ham (Ed.), Classification of Carbonate Rocks – A Symposium vol. 1, American Association of Petroleum Geologists, Tulsa, 1962, pp. 108–121.
[49] R.L. Folk, Spectral subdivision of limestone types, in: W.E. Ham (Ed.), Classification of Carbonate Rocks – A Symposium vol. 1, American Association of Petroleum Geologists, Tulsa, 1962, pp. 62–84.
[50] I.T. Jolliffe, Principal Component Analysis, in: Springer Series in Statistics, Springer- Verlag, New York, 2002.
[51] L.N. Warr, IMA-CNMNC approved mineral symbols, Mineralogical Magazine. 85 (2021) 291–320, https://doi.org/10.1180/mgm.2021.43.
[52] X. Chen, J. Li, Z. Lu, S. Ng, Y. Niu, J. Jiang, Y. Xu, Z. Lai, H. Liu, The role of brownmillerite in preparation of high-belite sulfoaluminate cement clinker, Appl. Sci. 12 (10) (2022) 1–12, https://doi.org/10.3390/app12104980.
[53] H.F.W. Taylor, Cement Chemistry, second ed., Thomas Telford Publishing, London, 1997.
[54] P. Reiterman, V. Davidová, M. Doleželová, P. Bauerová, M. Keppert, X-Ray diffraction study of hardening kinetics of natural hydraulic lime, International Multidisciplinary Scientific GeoConference: SGEM 19 (6.3) (2019) 379–386, https://doi.org/10.5593/sgem2019V/6.3.
[55] Z. Pavlík, M. Pavlikova, M. Záleská, M. Vyšvařil, T. Žižlavský, Lightweight thermal efficient repair mortars with expanded glass (EG) for repairing historical buildings: the effect of binder type and EG aggregate dosage on their performance, Energ. Buildings 276 (2022) 1–16, https://doi.org/10.1016/j.enbuild.2022.112526.
[56] I.P. Swainson, M.T. Dove, W.W. Schmahl, A. Putnis, Neutron powder diffraction study of the åkermanite-gehlenite solid solution series, Phys. Chem. Miner. 19 (1992) 185–195, https://doi.org/10.1007/BF00202107.
[57] M.L. Ligabue, A. Saburit, G. Lusvardi, D. Malferrari, J. García-Ten, E. Monfort, Innovative use of thermally treated cement-asbestos in the production of foaming materials: effect of composition, foaming agent, temperature and reaction time, Construct. Build Mater. 335 (2022) 1–9, https://doi.org/10.1016/j.conbuildmat.2022.127517.
[58] D. Moseley, F.P. Glasser, Properties and composition of bredigite-structured phases, J. Mater. Sci. 17 (1982) 2736–2740, https://doi.org/10.1007/BF00543911.
[59] C.E. Tilley, H.C.G. Vincent, The occurrence of an orthorhombic high-temperature form of Ca2SiO4 (bredigite) in the Scawt Hill contact-zone and as a constituent of slags (with plates XV and XVI.), Mineralogical magazine and journal of the Mineralogical Society 28 (200) (1948) 255–271, https://doi.org/10.1180/minmag.1948.028.200.02.
[60] B. Kostura, H. Kulveitová, J. Leško, Blast furnace slags as sorbents of phosphate from water solutions, Water Res. 39 (9) (2005) 1795–1802, https://doi.org/10.1016/j.watres.2005.03.010.
[61] P.A. Sabine, M.T. Styles, B.R. Young, The nature and paragenesis of natural bredigite and associated minerals from Carneal and Scawt Hill, Co. Antrim, Mineral. Mag. 49 (354) (1985) 663–670, https://doi.org/10.1180/minmag.1985.049.354.05.
[62] T. Sopcak, L. Medvecky, P. Jevinova, M. Giretova, A. Mahun, L. Kobera, R. Stulajterova, F. Kromka, V. Girman, M. Balaz, Physico-chemical, mechanical and antibacterial properties of the boron modified biphasic larnite/bredigite cements for potential use in dentistry, Ceram. Int. 49 (4) (2023) 6531–6544, https://doi.org/10.1016/j.ceramint.2022.10.119.
[63] J.D.C. McConnell, The hydration of larnite (β-Ca2SiO4) and bredigite (α1-Ca2SiO4) and the properties of the resulting gelatinous mineral plombierite, Mineral. Mag. J. Mineral. Soc. 30 (229) (1955) 672–680, https://doi.org/10.1180/minmag.1955.030.229.08.
[64] T.E. Bridge, Bredigite, larnite and γ dicalcium silicates from marble canyon, Am. Mineral. 51 (11–12) (1966) 1766–1774.
[65] Y.Q. Zhang, A.V. Radha, A. Navrotsky, Thermochemistry of two calcium silicate carbonate minerals: scawtite, Ca7(Si6O18)(CO3)·2H2O, and spurrite, Ca5(SiO4)2(CO3), Geochim. Cosmochim. Acta 115 (2013) 92–99, https://doi.org/10.1016/j.gca.2013.03.031.
[66] T. Matschei, B. Lothenbach, F.P. Glasser, The role of calcium carbonate in cement hydration, Cem. Concr. Res. 37 (4) (2007) 551–558, https://doi.org/10.1016/j.cemconres.2006.10.013.
[67] A. Arizzi, G. Cultrone, Mortars and plasters—how to characterise hydraulic mortars, Archaeol. Anthropol. Sci. 13 (144) (2021) 1–22, https://doi.org/10.1007/s12520-021-01404-2.
[68] J.I. Álvarez, R. Viega, S. Martínez-Ramírez, M. Secco, P. Faria, P.N. Maravelaki, M. Ramesh, I. Papayanni, J. Válek, RILEM TC 277-LHS report: a review on the mechanisms of setting and hardening of lime-based binding systems, Materials and Structures 54 (63) (2021) 1–30, https://doi.org/10.1617/s11527-021-01648-3.
[69] M. Secco, C. Previato, A. Addis, G. Zago, A. Kamsteeg, S. Dilaria, C. Canovaro, G. Artioli, J. Bonetto, Mineralogical clustering of the structural mortars from the Sarno Baths, Pompeii: a tool to interpret construction techniques and relative chronologies, J. Cult. Herit. 40 (2019) 265–273, https://doi.org/10.1016/j.culher.2019.04.016.
[70] M. Secco, S. Dilaria, J. Bonetto, A. Addis, S. Tamburini, N. Preto, G. Ricci, G. Artioli, Technological transfers in the Mediterranean on the verge of Romanization: insights from the waterproofing renders of Nora (Sardinia, Italy), Journal of Cultural Heritage 44 (2020) 63–82, https://doi.org/10.1016/j.culher.2020.01.010.
[71] S. Dilaria, M. Secco, J. Bonetto, G. Ricci, G. Artioli, Making ancient mortars hydraulic. How composition influences type and crystallinity of reaction products, in: V. Bokan Bosiljkov, A. Padovnik, T. Turk, P. Štukovnik (Eds.), Proceedings of the 6th Historic Mortars Conference - HMC 2022, Ljubljana, 2022, pp. 55–69.
[72] J. Ochoa-Franco, A. López-Díaz, Evaluation of the formation of andradite and carbonates of calcium in the synthesis of a geopolymer from white slag, Revista UIS Ingenierías 19 (4) (2020) 27–36, https://doi.org/10.18273/revuin.v19n4-2020003.
[73] C. Roosz, S. Grangeon, P. Blanc, V. Montouillout, B. Lothenbach, P. Henocq, E. Giffaut, P. Vieillard, S. Gaboreau, Crystal structure of magnesium silicate hydrates (M-S-H): the relation with 2:1 Mg–Si phyllosilicates, Cem. Concr. Res. 73 (2015) 228–237, https://doi.org/10.1016/j.cemconres.2015.03.014.
[74] E. Ruiz-Agudo, A. Cabello-González, S. Bonilla-Correa, C. Benavides-Reyes, M. Burgos-Ruiz, Estudio comparativo de materiales cementantes a base de CaO/MgO-SiO2, Macla: Revista de la Sociedad Española de Mineralogía 26 (2022) 172–173.
[75] M. Secco, Y. Asscher, G. Ricci, S. Tamburini, N. Preto, J. Sharvit, G. Artioli, Cementation processes of Roman pozzolanic binders from Caesarea Maritima (Israel), Construct. Build Mater. 355 (2022) 1–21, https://doi.org/10.1016/j.conbuildmat.2022.129128.
[76] P.F.G. Banfill, A.M. Foster, A relationship between hydraulicity and permeability of hydraulic lime, in: P. Bartos, C. Groot, J.J. Hughes (Eds.), International RILEM Workshop on Historic Mortars: Characteristics and Tests, RILEM Publications sarl, Cachan, 2000, pp. 173–183.
[77] J. Elsen, G. Mertens, R. Snellings, Portland cement and other calcareous hydraulic binders: History, production and mineralogy, in: G.E. Christidis (Ed.), Advances in the Characterization of Industrial Minerals, European Mineralogical Union Notes in Mineralogy vol. 9, 2011, pp. 441–479. London.
[78] P. Agrinier, A. Deutsch, U. Schärer, I. Martínez, Fast back-reactions of shock-released CO2 from carbonates: an experimental approach, Geochim. Cosmochim. Acta 65 (15) (2001) 2615–2632, https://doi.org/10.1016/S0016-7037(01)00617-2.
[79] N. Meller, C. Hall, A.C. Jupe, S.L. Colston, S.D. Jacques, P. Barnes, J. Phipps, The paste hydration of brownmillerite with and without gypsum: a time resolved synchrotron diffraction study at 30, 70, 100 and 150 °C, J. Mater. Chem. 14 (3) (2004) 428–435, https://doi.org/10.1039/B313215C.
[80] F. Massazza, Properties and applications of natural pozzolanas, in: J. Bensted, P. Barnes (Eds.), Structure and Performance of Cements, Second edition, SPON PRESS Taylor & Francis Group, New Fetter Lane, 2002, pp. 326–352.
[81] Saint Astier Website, Mineralogy & chemistry of raw materials and products. https://www.stastier.co.uk/mineralogy-chemistry-of-raw-materials-and-products/, 2022. Last access: 01/07/2022.
[82] K. Wang, L. Ren, L. Yang, Excellent carbonation behavior of Rankinite prepared by calcining the C-S-H: potential recycling of waste concrete powders for prefabricated building products, Materials 11 (8) (2018) 1–9, https://doi.org/10.3390/ma11081474.